Optics & Laser Technology 87 (2017) 79–86

Contents lists available at ScienceDirect

Optics & Laser Technology

journal homepage: www.elsevier.com/locate/optlastec

Full length article

Molecular orbital imaging for partially aligned molecules

Meiyan Qin [a], Xiaosong Zhu [b,*]

[a] Laboratory for Optical Information Technology, Wuhan Institute of Technology, Wuhan 430205, P.R. China
[b] School of Physics and Wuhan National Laboratory for Optoelectronics, Huazhong University of Science and Technology, Wuhan 430074, P.R. China

ARTICLE INFO

Article history:
Received 15 November 2015
Accepted 30 July 2016

Keywords:
High-order harmonic generation
Molecular orbital imaging
Molecular alignment

ABSTRACT

We investigate molecular orbital reconstruction using high-order harmonic emissions from partially aligned molecular ensembles. By carrying out the reconstruction procedure using the harmonic sampling with or without the spectral minimum, the roles of the harmonic phase and amplitude modulation due to the partial alignment can be separately studied. It is found that with the prior knowledge of the orbital symmetry, the reconstructed result is very sensitive to the modulation of the harmonic phase for the π_g orbital, while in the case of σ_g orbital, the reconstructed result is mainly determined by the harmonic amplitude. These results can provide an important reference for the future experiment of molecular orbital imaging.

© 2016 Elsevier Ltd. All rights reserved.

1. Introduction

Imaging structures and dynamics at different temporal and spatial scales is a major direction of modern science that encompasses physics, chemistry and biology [1–7]. Among the existing imaging technique, high-order harmonic spectroscopy (HHS) has been shown as an effective approach to resolving molecular structures and dynamics with unprecedented spatial and temporal resolutions [8–11]. Along with its another important application in producing coherent attosecond laser pulses in the soft x-ray range, high-order harmonic generation (HHG) has attracted a lot of interest in the past two decades [12–20]. The HHG occurs during the interaction of a strong laser field with a gas target and can be understood by a three-step model [21,22]. According to this model, an electron wavepacket (EWP) is first produced by laser ionization, then it is accelerated and driven back to the core by the laser field, and finally recombines with the parent ion to emit high-order harmonic photons. As the recolliding EWP has a duration of a few hundred attoseconds at recollision time, it gives rise to the attosecond temporal resolution of HHS. Meanwhile, the ultrashort de Broglie wavelength of the recolliding EWP allows for sub-Ångström spatial resolution.

An important method based on HHG to resolve molecular structure and dynamics with sub-Ångström and attosecond resolutions is the molecular orbital tomography (MOT), which was first proposed by J. Itatani et al. [23]. With this MOT scheme, a two-dimensional projection of the molecular orbital on the plane orthogonal to the pulse-propagation direction can be reconstructed [24–26]. In detail, by calibrating the harmonic signals from molecule aligned at various angles using that of a reference system with the same ionization energy, the recombination dipole matrix element of the molecular orbital is extracted. Then, by performing the inverse Fourier transform of the recombination dipole matrix elements, the target molecular orbital can be reconstructed. Note that in order to accurately extract the recombination dipole matrix element, the high-order harmonics from perfectly aligned molecules are needed. In experiments, however, the harmonic signals are generated from partially aligned molecular ensemble [27,28]. The measured harmonic signals are coherent superposition of the harmonic emissions at various alignment angles weighted by the angular distribution [11,24]. In most of previous works, these harmonic signals are treated as the harmonics generated from molecules purely aligned at the dominate angle in the MOT procedure to extract the dipole matrix element. Recently, it has been shown that the harmonic spectra, especially the spectral minimum position that contains important information on the molecular structure and dynamics, can be significantly modulated by the degree of alignment [29,30]. Hence, when the degree of alignment is changed the extracted dipole matrix element will be different. This may lead to a different reconstruction result. As the degree of alignment is sensitive to the experimental conditions, the degree of alignment achieved in different experiments is generally not the same. Hence, in order to better understand and compare the results obtained in different experiments, it is necessary to investigate how the degree of alignment affect the result of the orbital reconstruction.

* Corresponding author.
E-mail address: zhuxiaosong@hust.edu.cn (X. Zhu).

http://dx.doi.org/10.1016/j.optlastec.2016.07.019
0030-3992/© 2016 Elsevier Ltd. All rights reserved.

In this paper, molecular orbital tomography based on high-order harmonic generation from partially aligned molecular ensembles is investigated for molecules with different orbital symmetries and various degrees of alignment. By carrying out the reconstruction procedure using the harmonic sampling with or without the spectral minimum, the roles of the harmonic phase and amplitude modulation due to the partial alignment can be separately studied. It is found that with the prior knowledge of the orbital symmetry, the reconstructed result is very sensitive to the modulation of the harmonic phase for the π_g orbital, while in the case of σ_g orbital, the reconstructed result is mainly determined by the alignment-dependent harmonic amplitude.

2. Theoretical model

In our simulation, the complex amplitude of the harmonic signal at the delay τ with respect to the alignment pulse is calculated by

$$\tilde{\mathbf{S}}(\omega_n, \alpha) = \int_{\varphi'=0}^{2\pi} \int_{\theta'=0}^{\pi} \rho(\theta(\theta', \varphi', \alpha); \tau)\tilde{\mathbf{E}}(\omega_n, \theta', \varphi') \times \sin\theta' d\theta' d\varphi'. \quad (1)$$

Here, ω_n and α are the harmonic frequency and the angle between the alignment and probe pulse polarization, respectively. Linearly polarized alignment and probe pulses are used in our study. Both of them are set to propagate along the x axis of the laboratory frame, the polarization of the probe laser field is along the z axis of the laboratory frame. θ' and φ' are the polar and azimuthal angles in the frame of probe pulse, respectively. $\rho(\theta; \tau)$ is the time-dependent angular distribution in the frame of alignment pulse. It can be transformed to the frame of probe pulse using the relation $\cos\theta = \cos\alpha\cos\theta' + \sin\alpha\sin\theta'\cos\varphi'$. For clarity, a schematic illustration of our coordinate system is given in Fig. 1. As shown in this figure, the probe laser frame coincides with the laboratory frame and is fixed. The x axis of the probe and the alignment pulse frames are defined as the propagation direction of the two pulses. They coincide with each other. The z axis of the probe and the alignment pulse frames are defined by the polarization direction of their electric field, respectively. The alignment pulse frame is rotated about the x axis of the probe frame at an angle α.

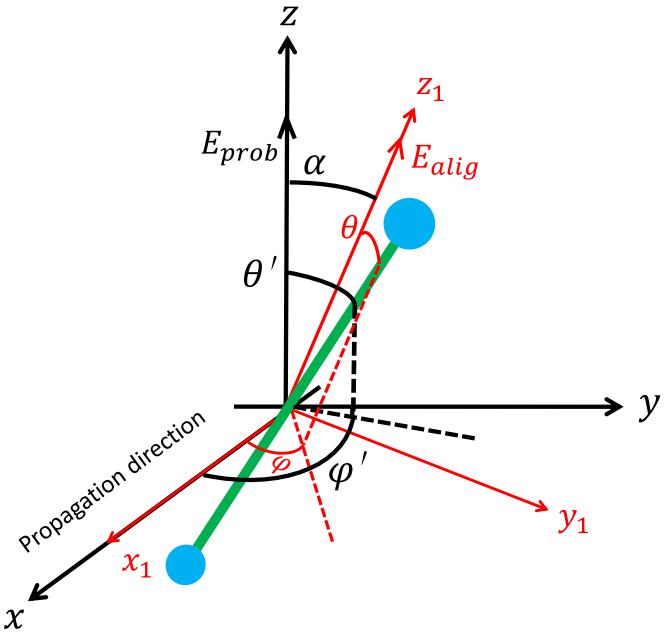

Fig. 1. A schematic illustration of our coordinate system.

By solving the time-dependent Schrödinger equation (TDSE) based on the rigid-rotor model [31,32], $\rho(\theta; \tau)$ can be calculated by

$$\rho(\theta; \tau) = \sum_{J_i} g(J_i) \sum_{M_i=-J_i}^{J_i} \int |\Psi^{J_i M_i}(\theta, \varphi; \tau)|^2 d\varphi, \quad (2)$$

where $\Psi^{J_i M_i}(\theta, \varphi; \tau)$ is the rotational wavepacket corresponding to the initial state $|J_i, M_i\rangle$. $g(J_i) = Q(J_i)/(\sum_{J=0}^{J_{max}}(2J+1)Q(J))$ with $Q(J_i) = \exp[-BJ_i(J_i+1)/(k_BT)]$ being the Boltzmann distribution function of the initial field-free state $|J_i, M_i\rangle$ at temperature T. $\tilde{\mathbf{E}}(\omega_n, \theta', \varphi')$ is the complex amplitude of the high-order harmonics generated from the molecule aligned at θ' with respective to the polarization of the probe laser pulse. It is calculated by using the strong-field approximation (SFA) model for molecules within the single-active-electron (SAE) approximation [21]. Generally, $\tilde{\mathbf{E}}(\omega_n, \theta', \varphi')$ has two components, $\tilde{E}_z$ and $\tilde{E}_y$, which are parallel and perpendicular to the probe pulse polarization, respectively [33]. As a result, the observed harmonic signal $\mathbf{S}(\omega_n, \alpha)$ also has two components $S_z(\omega_n, \alpha)$ and $S_y(\omega_n, \alpha)$. In experiment, these two components can be separately collected by a silver-coated mirror acting as a polarizer [34] or an XUV reflective polarizer consisting of three fused-silica blanks [35,36]. In our simulation, the complex amplitude of the z component $\tilde{S}_z(\omega_n, \alpha)$ is used to reconstruct the molecular orbital [37]. The corresponding $\tilde{E}_z$ is calculated based on the velocity form of the transition dipole, which is better suited to quantify the recombination step in molecular HHG [38]. Since small linear molecules are considered in our work, $\tilde{E}_z(\omega_n, \theta')$ is φ'-independent [33]. More details about our calculation of $\tilde{E}_z(\omega_n, \theta')$ and $\rho(\theta; \tau)$ can be found in our previous works [39,40].

By fixing the delay time τ at the first half revival and rotating the polarization of the alignment pulse with respect to that of the probe pulse, the harmonic signals for a set of angles α can be obtained. Using these harmonic signals, the molecular orbital can be reconstructed by following the MOT procedure. In our simulation, the reconstruction of molecular orbital is performed in the velocity form. Hence, the dipole velocity is extracted from the harmonic signals by using [37]

$$\mathbf{d}^V(\mathbf{k}, \alpha) = \frac{1}{\eta(\alpha)} \frac{\tilde{S}_z(\omega_n, \alpha)}{\tilde{S}_z^{ref}(\omega_n)} \mathbf{d}_{ref}^V(\mathbf{k}), \quad (3)$$

where $\tilde{S}_z^{ref}(\omega_n)$ and $\mathbf{d}_{ref}^V(\mathbf{k})$ are the complex amplitude of the harmonics and the dipole velocity of the reference atom, respectively. $\mathbf{d}_{ref}^V(\mathbf{k})$ is calculated by $\mathbf{d}_{ref}^V(\mathbf{k}) = i\omega_n \mathbf{d}_{ref}^L(\mathbf{k})$ where $\mathbf{d}_{ref}^L(\mathbf{k}) = i\left(\frac{2^{7/2}(2I_p)^{5/4}}{\pi}\right)\frac{\mathbf{k}}{(\mathbf{k}^2+2I_p)^3}$ and I_p equals to the ionization energy of the corresponding target molecular orbital. $\mathbf{k}$ represents the electron wavevector at the recollision instant. It is related to the harmonic energy by $\omega_n = \mathbf{k}^2/2$. $\eta(\alpha)$ is the k-independent scaling factor. After obtaining the dipole velocity, the molecular orbital is reconstructed by

$$\tilde{\Psi}^D(y, z) = \mathcal{F}_{k\to r}\left[\frac{d_z^V(k_y, k_z)}{k_z}\right]. \quad (4)$$

By performing the same procedure for various degrees of alignment, the effect of molecular alignment on the molecular orbital tomography is investigated.

3. Results and discussions

We use CO_2 and N_2 molecules as the examples to study the molecular orbital reconstruction with high-order harmonic emission from partially aligned molecules. The highest occupied

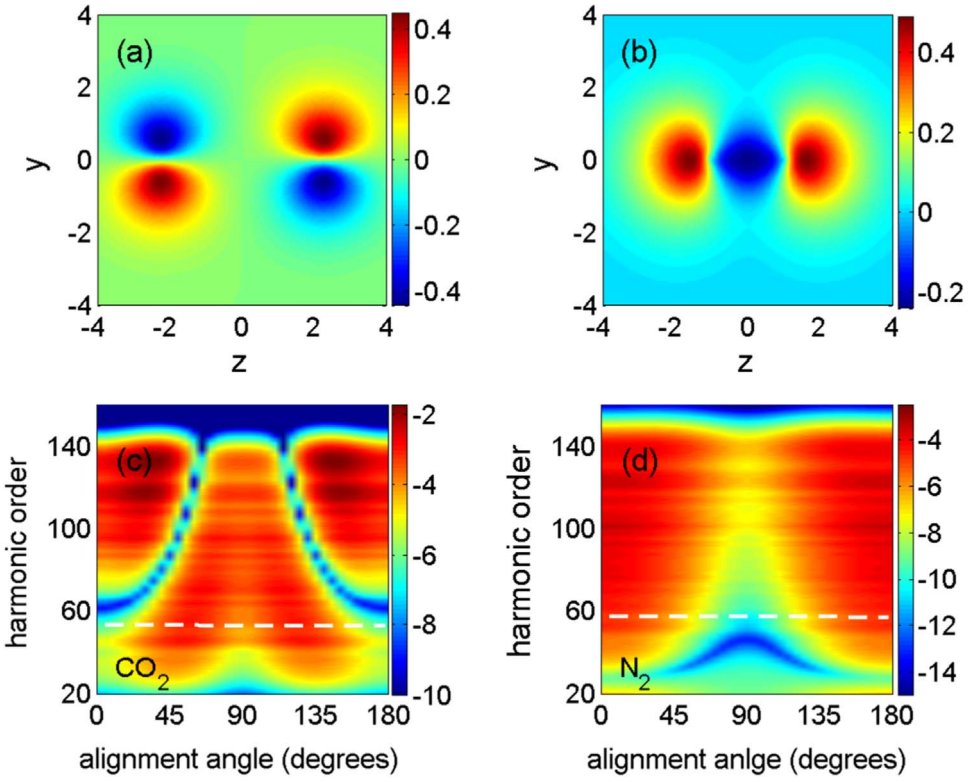

Fig. 2. (a–b) Two-dimensional projection of the HOMO for CO_2 molecule (panel a) and for N_2 molecule (panel b). They are obtained using the Gaussian 03 ab initio code. (c–d) The harmonic spectra from partially aligned CO_2 molecule with $\langle \cos^2\theta \rangle$ as 0.78 (panel c) and N_2 molecule with $\langle \cos^2\theta \rangle$ as 0.76 (panel d).

molecular orbitals (HOMO) of CO_2 and N_2 molecules are shown in Fig. 2(a) and (b), respectively. These molecular orbitals are obtained by using the Gaussian 03 ab initio code [41]. As shown in Fig. 2(a) and (b), the HOMOs of CO_2 and N_2 molecules possess different symmetries, i.e. π_g and σ_g symmetries, respectively. In our simulation, a 100-fs pump pulse is used to align the CO_2 and N_2 molecules. The rotational temperatures of the two molecules are set to be 40 K. By varying the intensity of the pump pulse, various degrees of alignment are achieved. The degree of alignment is characterized by the alignment parameter $\langle \cos^2\theta \rangle$, i.e. the expectation value of $\cos^2\theta$. To generate high harmonic emissions from the two molecules with various degrees of alignment, an 18-fs 1450-nm probe pulse with an intensity of 1.7×10^{14} W/cm^2 is used. We define the angle α between the pump and probe pulses as the alignment angle. In Fig. 2, the harmonic spectra from partially aligned CO_2 molecule with $\langle \cos^2\theta \rangle$ as 0.78 (panel c) and N_2 molecule with $\langle \cos^2\theta \rangle$ as 0.76 (panel d) are presented as a function of the harmonic order and the alignment angle. As shown in Fig. 2(c) and (d), obvious spectral minima are observed in the maps of the harmonic spectra for the two molecules. Moreover, the maps of the harmonic spectrum of the two molecules can be divided into two parts with or without spectral minimum, as separated by the white dashed lines in Fig. 2(c) and (d). On one hand, the spectral width of the high-order harmonic spectrum observed in experiment is limited. The exact position of the limited spectral window is crucial to recovering the structure of the molecular orbital [37]. Hence it is very necessary to investigate the influence of the imperfect alignment on the orbital reconstruction using different parts of the spectrum. On the other hand, the modulation of the harmonic spectrum due to the degree of molecular alignment is more significant near the spectral minimum, because the minimum position can be drastically shifted by varying the degree of alignment. Based on the above two points, the harmonic sampling with or without the spectral minimum are considered in our work. As one can see later, this enables us to separately study the roles of the harmonic phase and amplitude modulation due to the partial alignment.

In Fig. 3, the reconstructed orbitals of CO_2 molecule for three different degrees of alignment are presented. The corresponding angular distributions and the values of $\langle \cos^2\theta \rangle$ are shown in the first row of Fig. 3. The results presented in the second and third rows of Fig. 3 correspond to the harmonic sampling without and with spectral minimum, respectively. For comparison, the spectral widths of the harmonic sampling without and with spectral minimum are the same, which are the harmonics from 21 to 41 orders and from 61 to 81 orders, respectively. The step of the angular sampling is $\Delta\alpha = 5^\circ$. A phase jump of π is imposed on the extracted dipole velocity at $\alpha = 90^\circ$ due to the orbital symmetry of CO_2 molecule. As shown in the second row of Fig. 3, the main structure of the HOMO of CO_2 molecule is reproduced using the harmonic sampling without spectral minimum, even for the case that the angular distribution is almost isotropic, as shown in Fig. 3 (d). One can also find an interesting phenomenon that the reconstructed orbitals are almost the same for the three different degrees of alignment, i.e. the reconstruction result is independent of the degree of alignment. As for the harmonic sampling with spectral minimum shown in the third row of Fig. 3, the main structure of the HOMO of CO_2 molecule is also reproduced for the three different degrees of alignment, despite some extra oscillations resulting from the higher energy of the harmonic sampling [37]. Different from those of the harmonic sampling without spectral minimum, the result of the reconstruction using the harmonic signals with spectral minimum varies obviously with the degree of alignment. As shown in Fig. 3(g–i), obvious shrinkage in the y direction is observed, meanwhile the reconstructed orbital elongates in the z direction as increasing the degree of alignment.

Because the molecular orbital is obtained by performing the inverse Fourier transform of the dipole velocity, the variation of the reconstructed orbital originates from the modulation of the

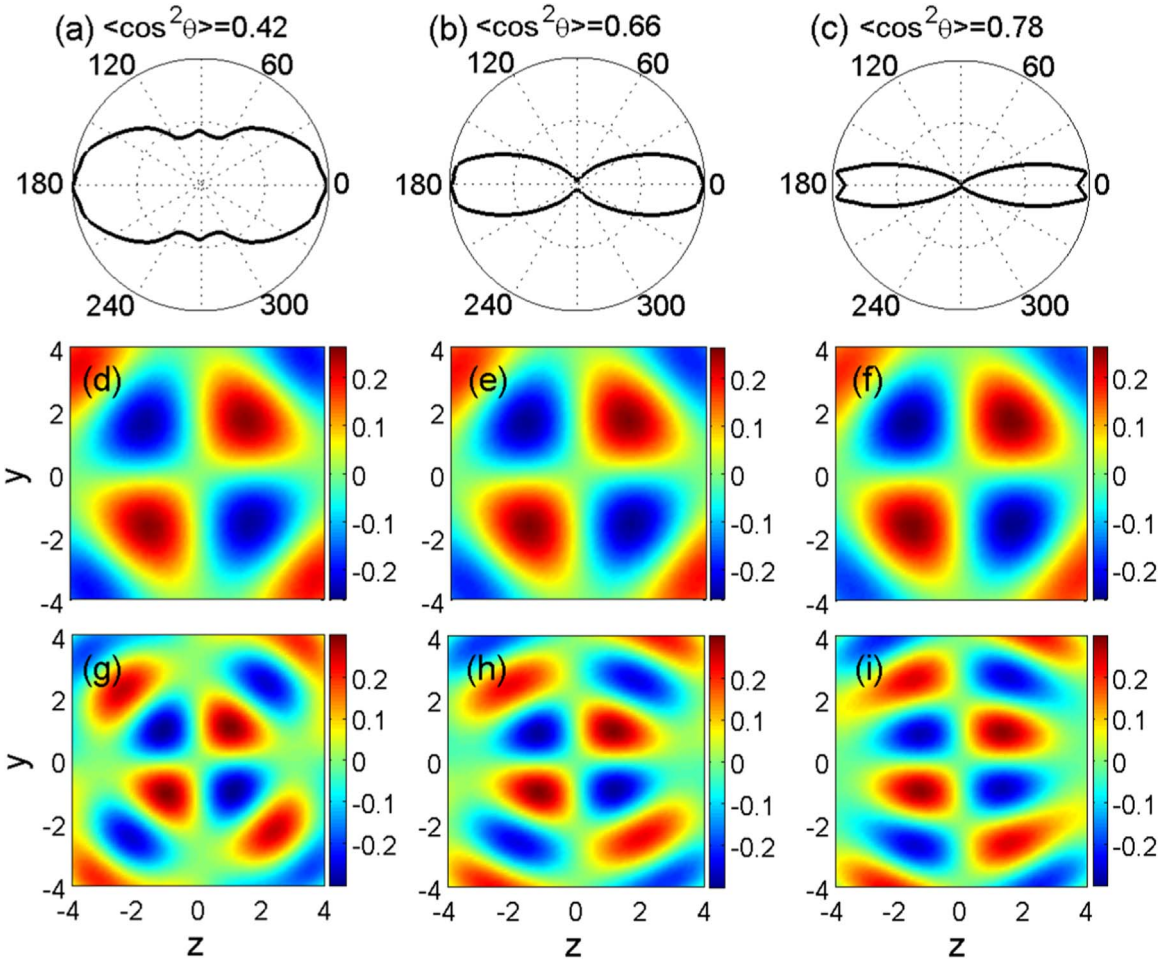

Fig. 3. (a–c) The angular distribution of CO_2 molecule with $\langle \cos^2\theta \rangle$ as 0.42 (panel a), 0.66 (panel b), and 0.78 (panel c). (d–i) The reconstructed orbitals of CO_2 for the three different degrees of alignment. The results in the second and third rows correspond to the harmonic sampling from the harmonics 21 to 41 orders without the spectral minimum and from the harmonics 61–81 orders with the spectral minimum, respectively.

dipole velocity. Hence, we perform an analysis of the extracted dipole velocity in the two cases of the harmonic sampling, to get an insight into the influence of the degree of alignment on the reconstruction of the HOMO of the CO_2 molecule. The amplitudes and phases of the extracted dipole velocities of the reconstructed orbitals in Fig. 3 are presented in Fig. 4. The results for the harmonic sampling without and with spectral minimum are presented in the first two and the last two rows of Fig. 4, respectively. The first, second, and third columns represent the three different degrees of alignment with $\langle \cos^2\theta \rangle$ as 0.42, 0.66, and 0.78, respectively. As shown in Fig. 4(a1–a3) for the harmonic sampling without spectral minimum, the angular distribution of the amplitude of the dipole velocity varies significantly with increasing the degree of alignment. This modulation of the amplitude induced by the degree of alignment does not affect the reconstruction result, as shown in Fig. 3(d–f). On the contrary, the reconstruction result is sensitive to the modulation of the phase of the dipole velocity. When the phases of the dipole velocity are almost the same for different degrees of alignment, as shown in the case of the harmonic sampling without spectral minimum in Fig. 4(b1–b3), the reconstructed orbitals also remain the same, as shown in Fig. 3(d–f). When the phases of the dipole velocity vary obviously with the degree of alignment due to the alignment-induced shift of the spectral minimum position, as shown in the case of the harmonic sampling with spectral minimum in Fig. 4(c1–c3), the reconstructed orbital correspondingly varies with the degree of alignment, as shown in Fig. 3(g–i). Hence the modulation of the angular distribution of the dipole velocity amplitude has few influences on the reconstruction result of the HOMO of CO_2 molecule, the modulation of the dipole velocity phase determines the variation of the reconstructed orbital.

This can be explained by the symmetry of the HOMO of CO_2 molecule. Because the HOMO of CO_2 molecule possesses π_g symmetry, there is a π phase jump of the dipole velocity at 90° for all the harmonic orders. Hence in the inverse Fourier transform of the dipole velocity, the integral over the alignment angle is destructive. Additionally, the angular distribution of the amplitude of the dipole velocity is symmetric about the alignment angle at 90°. As a result, the angular distribution of the dipole velocity amplitude is smoothed away after the integral. Therefore for the π_g orbital, the reconstruction is not sensitive to the modulation of the angular distribution of the dipole velocity amplitude. The variation of the reconstructed orbital with the degree of alignment is mainly determined by the modulation of the dipole velocity phase.

We also investigate the effect of molecular alignment on the reconstruction of the HOMO of N_2 molecule, which possesses σ_g symmetry. The reconstruction results for three different degrees of alignment are presented in Fig. 5. The corresponding angular distributions and values of $\langle \cos^2\theta \rangle$ are shown in the first row of Fig. 5. The reconstructed orbitals presented in the second and third rows correspond to the harmonic sampling from 61 to 71 orders without spectral minimum and from 37 to 47 orders with spectral

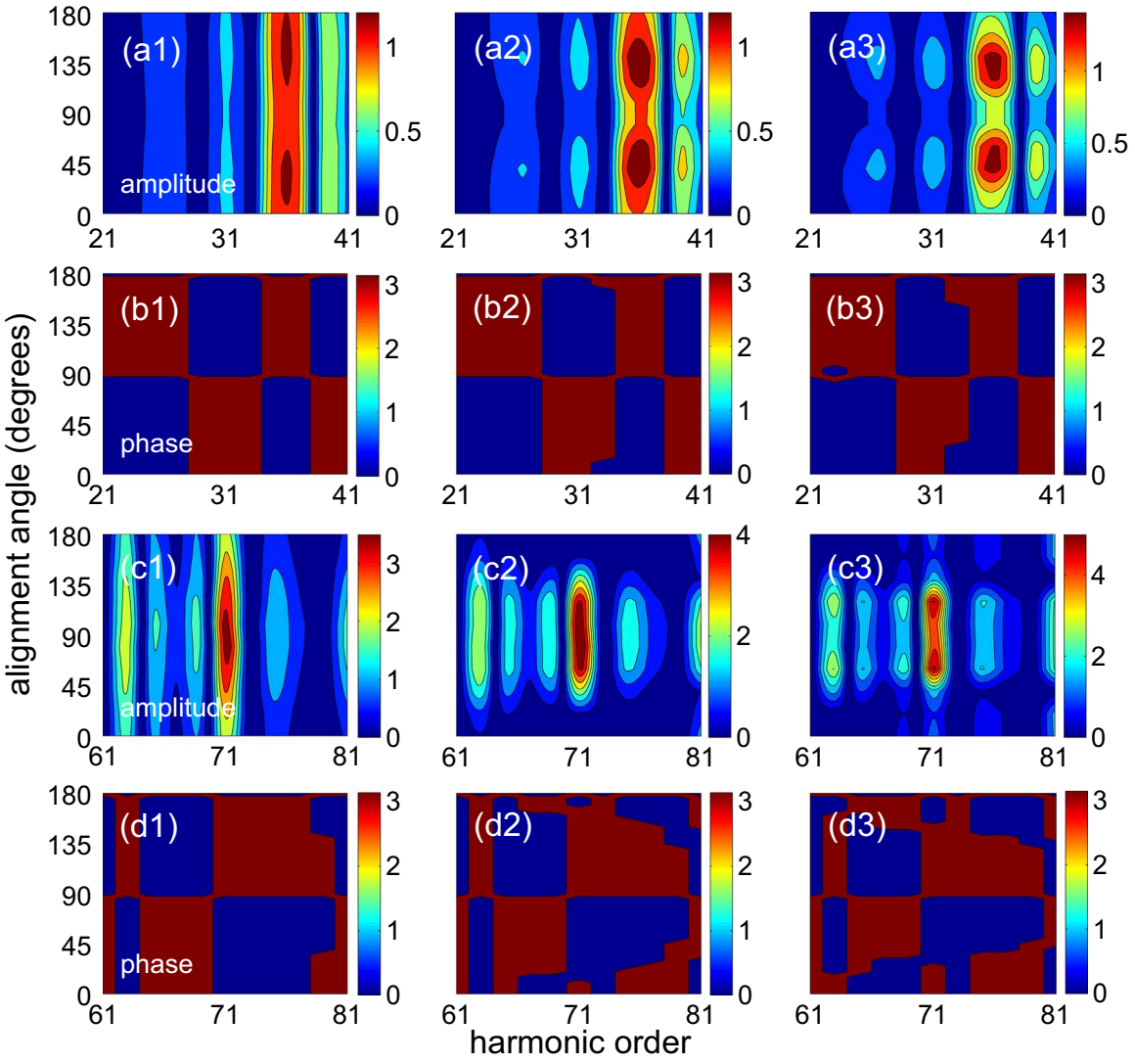

Fig. 4. The amplitudes and phases of the extracted dipole velocities of the orbitals in Fig. 3 for CO_2 molecule. The results presented in the first and second rows correspond to the orbitals in the second row of Fig. 3, while those in the third and forth rows correspond to the orbitals in the third row of Fig. 3. The first, second, and third columns represent the degree of alignment with $\langle \cos^2\theta \rangle$ as 0.42, 0.66, and 0.78, respectively.

minimum, respectively. As shown in Fig. 5(d–f) and (g–i), the reconstructed orbital of the N_2 molecule varies significantly with the degree of alignment in both two cases of the harmonic sampling. When the angular distribution is nearly an isotropic distribution ($\langle \cos^2\theta \rangle = 0.37$), the reconstructed orbitals only possess the symmetry of the HOMO of N_2 molecule but its essential structure is missing, as shown in the first column of Fig. 5. When the alignment parameter increases to 0.76, the orbital is very similar to the one reconstructed using the harmonics from perfectly aligned molecules.

In the following, the variation of the extracted dipole velocities with the degree of alignment is analyzed for the N_2 molecule. In Fig. 6, the amplitudes and phases of the extracted dipole velocities of the reconstructed orbitals in Fig. 5 are presented. As shown in Fig. 6(a1–a3) and (b1–b3) for the harmonic sampling without the spectral minimum, the angular distribution of the amplitude of the dipole velocity varies significantly with increasing the degree of alignment, while the phase of the dipole velocity remain the same. In the case of the harmonic sampling with spectral minimum shown in Fig. 6(c1–c3) and (d1–d3), both the angular distribution of the amplitude and the phase of the dipole velocity vary with the degree of alignment, due to the shift of the spectral minimum position with the degree of alignment. Moreover, one can notice that the modulations of the angular distribution of the dipole velocity amplitude present a similar pattern in the two cases of the harmonic sampling, i.e. the ratio between the amplitude of the dipole velocity at the alignment angles 0° and 90° increases with the degree of alignment, as shown in Fig. 6(a1–a3) and (c1–c3). As the orbital is obtained by performing the inverse Fourier transform of the dipole velocity, the variation of the reconstructed orbital can only originates from the modulations of the amplitude and the phase of the dipole velocity. Hence in the case of the harmonic sampling without spectral minimum, the variation of the reconstructed orbital results from the variation of the angular distribution of the dipole velocity amplitude. In the case of the harmonic sampling with spectral minimum, although the phase of the dipole velocity varies obviously with the degree of alignment, the reconstructed orbital still varies in a similar pattern to that of the harmonic sampling without spectral minimum, as shown in Fig. 5 (d–f) and (g–i). Hence, similar to the case of the harmonic sampling without the spectral minimum, the variation of the reconstructed orbital shown in Fig. 5(g–i) also mainly results from

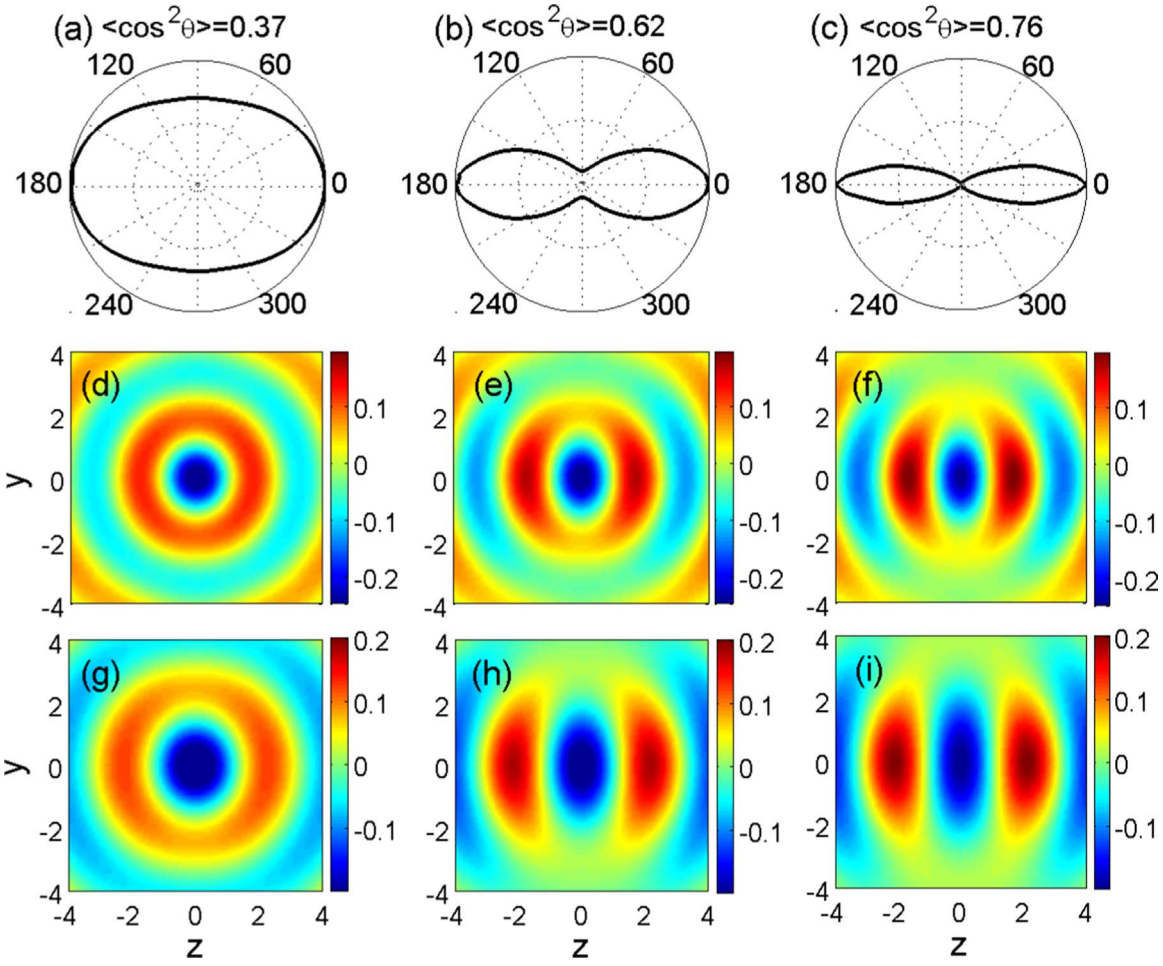

Fig. 5. (a–c) The angular distribution of N_2 molecule with $\langle \cos^2\theta \rangle$ as 0.37 (panel a), 0.62 (panel b), and 0.76 (panel c). (d–i) The reconstructed orbitals of N_2 for the three different degrees of alignment. The results in the second and third rows correspond to the harmonic sampling from the harmonics 61 to 71 orders without the spectral minimum and from the harmonics 37 to 47 orders with the spectral minimum, respectively.

the modulation of the angular distribution of the dipole velocity amplitude. The modulation of the dipole velocity phase plays few roles in the influence of the degree of alignment on the reconstruction of the HOMO of N_2 molecule.

This can be explained by the symmetry of the HOMO of N_2 molecule. Because the HOMO of N_2 molecule possesses σ_g symmetry, the angular distribution of both the amplitude and the phase of the dipole velocity are symmetric about the alignment angle at 90°. In the inverse Fourier transform of the dipole velocity, the integral over the alignment angle is constructive. Hence the modulation of the angular distribution of the dipole velocity amplitude is not smoothed out after the integral. This leads to the sensitivity of the reconstructed orbital to the modulation of the angular distribution of the dipole velocity amplitude. In contrast, the influence of the variation of the dipole velocity phase is comparably small. Hence for the σ_g orbital, the variation of the reconstructed orbital with the degree of alignment mainly result from the modulation of the angular distribution of the dipole velocity amplitude.

4. Conclusion

In summary, we carry out the MOT procedure using the harmonic signals generated from partially aligned molecules with various degrees of alignment. The molecular orbitals possessing π_g and σ_g symmetries are considered. It is found that the influence of the degree of alignment on the result of the MOT depends on the orbital symmetry and the harmonic sampling range. In the case of the π_g orbital, the dipole velocity is antisymmetric about the alignment angle 90°. The modulation of the angular distribution of the dipole velocity amplitude is smoothed out after the inverse Fourier transform of the dipole velocity. Hence the reconstruction result is not sensitive to the modulation of the angular distribution of the dipole velocity, the variation of the reconstruction orbital with the degree of alignment is mainly determined by the modulation of the dipole velocity phase. For the σ_g orbital, the dipole velocity is symmetric about the alignment angle 90°. The modulation of the angular distribution of the dipole velocity amplitude is not smoothed out after the inverse Fourier transform. Hence, the reconstruction result is very sensitive to the modulation of the angular distribution of the dipole velocity amplitude. In contrast, the influence of the variation of the dipole velocity phase is comparably small. When the harmonic sampling without spectral minimum, only the angular distribution of the dipole velocity amplitude varies significantly with the degree of alignment. When the harmonic sampling with spectral minimum, both the angular distribution of the dipole velocity amplitude and the dipole velocity phase vary obviously with the degree of alignment. Therefore, the reconstruction result of the π_g orbital using the harmonic signals without spectral minima are alignment independent, while those using the harmonic sampling with spectral minima become

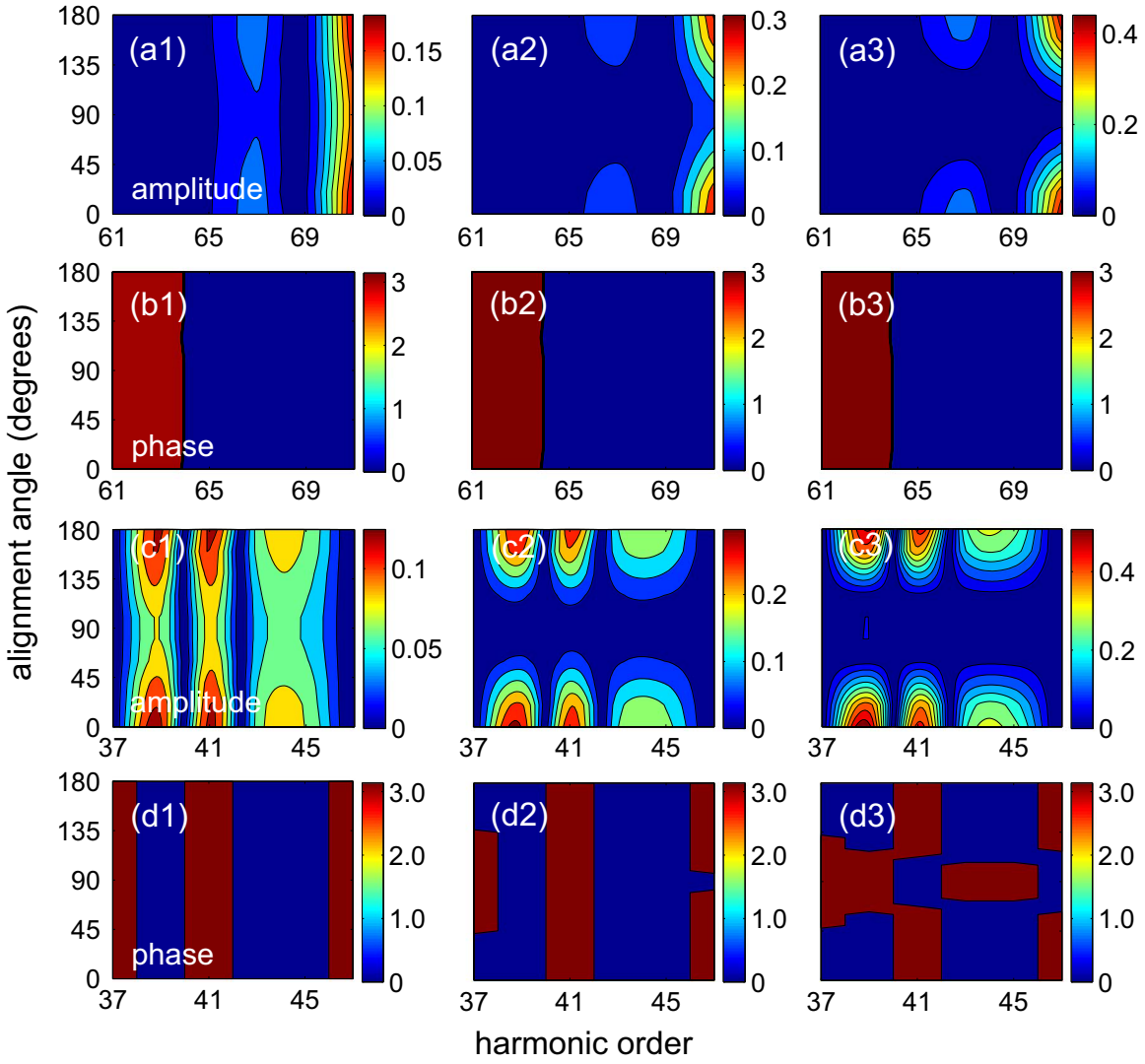

Fig. 6. The amplitudes and phases of the extracted dipole velocities of the orbitals in Fig. 5 for N_2 molecule. The results presented in the first and second rows correspond to the orbitals in the second row of Fig. 5, while those in the third and forth rows correspond to the orbitals in the third row of Fig. 5. The first, second, and third columns represent the degree of alignment with $\langle \cos^2\theta \rangle$ as 0.37, 0.62, and 0.76, respectively.

alignment dependent. As for the σ_g orbital, the reconstructed results are sensitive to the degree of alignment, irrespective of the harmonic sampling range.

Acknowledgements

This work was supported by the National Natural Science Foundation of China under Grants No. 11234004 and 11404123, the Natural Science Foundation of Hubei Province of China under Grants No. 2014CFB174. Numerical simulations presented in this paper were carried out using the High Performance Computing Center experimental testbed in SCTS/CGCL (see http://grid.hust.edu.cn/hpcc).

References

[1] H.J. Wöner, J.B. Bertrand, D.V. Kartashov, et al., Following a chemical reaction using high-harmonic interferometry, Nature 466 (2010) 604–607.
[2] Q. Liao, Y. Zhou, C. Huang, et al., Multiphoton Rabi oscillations of correlated electrons in strong-field nonsequential double ionization, New J. Phys. 14 (2012) 013001.
[3] F. Calegari, D. Ayuso, A. Trabattoni, et al., Ultrafast electron dynamics in phenylalanine initiated by attosecond pulses, Science 346 (2014) 336–339.
[4] Y. Zhou, C. Huang, Q. Liao, et al., Classical simulations including electron correlations for sequential double ionization, Phys. Rev. Lett. 109 (2012) 053004.
[5] X. Lai, C. Wang, Y. Chen, et al., Elliptical polarization favors long quantum orbits in high-order above-threshold ionization of noble gases, Phys. Rev. Lett. 110 (2013) 043002.
[6] M. Li, P. Zhang, S. Luo, et al., Selective enhancement of resonant multiphoton ionization with strong laser fields, Phys. Rev. A 92 (2015) 063404.
[7] Y. Li, M. Qin, X. Zhu, et al., Ultrafast molecular orbital imaging based on attosecond photoelectron diffraction, Opt. Express 23 (2015) 10687.
[8] M. Lein, Attosecond probing of vibrational dynamics with high-harmonic generation, Phys. Rev. Lett. 94 (2005) 053004.
[9] O. Smirnova, Y. Mairesse, S. Patchkovskii, et al., High harmonic interferometry of multi-electron dynamics in molecules, Nature 460 (2009) 972–977.
[10] S.R. Leone, C.W. McCurdy, J. Burgdörfer, et al., What will it take to observe processes in 'real time'? Nat. Photonics 8 (2014) 162–166.
[11] R. Torres, N. Kajumba, J.G. Underwood, et al., Probing orbital structure of polyatomic molecules by high-Order harmonicgeneration, Phys. Rev. Lett. 98 (2007) 203007.
[12] Y. Mairesse, A. de Bohan, L.J. Frasinski, et al., Attosecond synchronization of high-harmonic soft x-rays, Science 302 (2003) 1540–1543.
[13] P. Lan, P. Lu, W. Cao, et al., Isolated sub-100-as pulse generation via controlling electron dynamics, Phys. Rev. A 76 (2007) 011402(R).
[14] W. Cao, P. Lu, P. Lan, et al., Efficient isolated attosecond pulse generation from a multi-cycle two-color laser field, Opt. Express 15 (2007) 530.
[15] M. Chini, K. Zhao, Z. Chang, The generation, characterization and applications of broadband isolated attosecond pulses, Nat. Photonics 8 (2014) 178–186.
[16] X. Zhu, M. Qin, Q. Zhang, et al., Role of the Coulomb potential on the ellipticity in atomic high-orderharmonics generation, Opt. Express 20 (2012) 16275–16284.

[17] J. Luo, Y. Li, Z. Wang, et al., Ultra-short isolated attosecond emission in mid-infrared inhomogeneous fields without CEP stabilization, J. Phys. B: At. Mol. Opt. Phys. 46 (2013) 145602.
[18] L. He, P. Lan, Q. Zhang, et al., Spectrally resolved spatiotemporal features of quantum paths in high-order-harmonic generation, Phys. Rev. A 92 (2015) 043403.
[19] M. Chini, X. Wang, Y. Cheng, et al., Coherent phase-matched VUV generation by field-controlled bound states, Nat. Photonics 8 (2014) 437–441.
[20] X. Zhu, X. Liu, Y. Li, et al., Molecular high-order-harmonic generation due to the recollision mechanism by a circularly polarized laser pulse, Phys. Rev. A 91 (2015) 043418.
[21] M. Lewenstein, ph. Balcou, M.Yu. Ivanov, et al., Theory of high-harmonic generation by low-frequency laser fields, Phys. Rev. A 49 (1994) 2117–2132.
[22] P.B. Corkum, Plasma perspective on strong field multiphoton ionization, Phys. Rev. Lett. 71 (1993) 1994–1997.
[23] J. Itatani, J. Levesque, D. Zeidler, et al., Tomographic imaging of molecular orbitals, Nature 432 (2004) 867–871.
[24] S. Haessler, J. Caillat, W. Boutu, et al., Attosecond imaging of molecular electronic wave packets, Nat. Phys. 6 (2010) 200–206.
[25] C. Vozzi, M. Negro, F. Calegari, et al., Generalized molecular orbital tomography, Nat. Phys. 7 (2011) 822–826.
[26] X. Zhu, M. Qin, Y. Li, et al., Tomographic reconstruction of molecular orbitals with twofold mirror antisymmetry: overcoming the nodal plane problem, Phys. Rev. A 87 (2013) 045402.
[27] H. Stapelfeldt, T. Seideman, Aligning molecules with strong laser pulses, Rev. Mod. Phys. 75 (2003) 543–557.
[28] S.J. Weber, M. Oppermann, J.P. Marangos, Role of rotational wave packet in strong field experiments, Phys. Rev. Lett. 111 (2013) 263601.
[29] C. Jin, A.T. Le, C.D. Lin, Analysis of effects of macroscopic propagation and multiple molecular orbitals on the minimum in high-order harmonic generation of aligned CO_2, Phys. Rev. A 83 (2011) 053409.
[30] A. Rupenyan, P.M. Kraus, J. Schneider, et al., High-harmonic spectroscopy of isoelectronic molecules: Wavelength scaling of electronic-structure and multielectron effects, Phys. Rev. A 87 (2013) 033409.
[31] J. Ortigoso, M. Rodriguez, M. Gupta, B. Friedrich, Time evolution of pendular states created by the interaction of molecular polarizability with a pulsed nonresonant laser field, J. Chem. Phys. 110 (1999) 3870–3875.
[32] T. Seideman, Revival structure of aligned rotational wave packets, Phys. Rev. Lett. 83 (1999) 4971–4974.
[33] M. Lein, R.D. Nalda, E. Heesel, et al., Signatures of molecular structure in the strong-field response of aligned molecules, J. Mod. Opt. 52 (2004) 465–478.
[34] P. Antoine, B. Carre, A. L'Huillier, M. Lewenstein, Polarization of high-order harmonics, Phys. Rev. A 55 (1997) 1314–1324.
[35] A. Fleischer, O. Kfir, T. Diskin, P. Sidorenko, O. Cohen, Spin angular momentum and tunable polarization in high-harmonic generation, Nat. Photon-. 8 (2014) 543–549.
[36] G. Lambert, B. Vodungbo, J. Gautier, et al., Towards enabling femtosecond helicity-dependent spectroscopy with high-harmonic sources, Nat. Commun. 8 (2015) 6167.
[37] S. Haessler, J. Caillat, P. Salières, Self-probing of molecules with high harmonic generation, J. Phys. B: At. Mol. Opt. Phys. 44 (2011) 203001.
[38] C.C. Chirilă, M. Lein, Assessing different forms of the strong-field approximation for harmonicgeneration in molecules, J. Mod. Opt. 54 (2007) 1039–1045.
[39] M. Qin, X. Zhu, Y. Li, et al., Interference of high-order harmonics generated from molecules at different alignment angles, Phys. Rev. A 89 (2014) 013410.
[40] M. Qin, X. Zhu, Y. Li, et al., Probing rotational wave-packet dynamics with the structural minimum in high-order harmonic spectra, Opt. Express 22 (2014) 6362–6371.
[41] M.J. Frisch, G.W. Trucks, H.B. Schlegel, et al., Gaussian 03, Revision C.02, Gaussian Inc., Wallingford, CT, 2010.